JOURNAL INDIAN ASSOCIATION OF SEDIMENTOLOGISTS ISSN NO 2582 – 2020
Vol. 39, Issue 2, 2022, pp. 30-46
DOI: https://doi.org/10.51710/jias.v39iII.256

Geochemical Evolution of Dolomites in Thanagazi Formation of Mesoproterozoic Alwar Basin, Northwest India

R. Sajeev, Dinesh Pandit*and Mallickarjun Joshi

Department of Geology, Institute of Science, Banaras Hindu University, Varanasi - 221005, India
**Corresponding author:dpandit@hotmail.com*

Abstract

The geochemistry of dolomite in part of the Thanagazi Formation in the Mesoproterozoic Alwar Basin has been studied employing major and trace elements, including rare earth elements (REEs) to understand their provenance and paleoweathering conditions. In the current study, two distinct types of dolomites were identified viz. amorphous and crystalline. Various geochemical discriminants such as SiO_2 vs Al_2O_3 and CaO vs MgO indicate that the dolomites were originated from sedimentary sources with substantial metasomatic and biogenic contributions. Geochemical constraints from plots of Fe_2O_3/Al_2O_3 vs. $Al_2O_3/(Al_2O_3+Fe_2O_3)$ and rare earth element compositions for provenance signatures suggest likely deposition of dolomites in shallow marine sedimentary environment. Based on geothermometric estimates and base metal concentrations in dolomites, it is inferred that the mixing of sediments derived from two different sources (metasomatic and biogenic) were likely responsible for the dolomitization in the Thanagazi Formation of the Mesoproterozoic Alwar Basin.

Keywords*:* Alwar, Dolomite,Diagenesis, Geochemistry, Sedimentary Provenance

Introduction

Dolomite is a carbonate mineral in the ancient platforms and is mostly associated with hypersaline brines or schizohaline waters or the long-term circulation of seawater through platform sediments (Land, 1985; Hardie, 1987; Warren, 2000). Geochemical constraints (salinity, temperature, pressure, etc.) probably affect the nature of carbonate precipitation from the waters, whereas the variation in the relative amounts of magnesium and calcium is particularly important (Alderman and Borch, 1963; Baithwaite, 1991; Bouton et al., 2020). Dolomite is one of the thermodynamically stable carbonate phases in ocean water and an extremely common constituent of ancient terrestrial carbonate rocks (Baker and Kastner, 1981; Lee and Lindgren, 2015). Precambrian carbonates are characteristically dolomitic in composition and associated with prevalent secondary silicification (Eriksson and Warren, 1983). Widespread occurrences of Precambrian dolomite were precipitated from seawater during diagenesis (Tucker, 1982) or late-stage dolomitization by penetrating ground waters in burial diagenetic settings i.e., penecontemporaneous dolomites (Machel, 2004). Hydrothermal dolomites are commonly crystallized from hydrothermal fluids in a diagenetic stage (Boni et al., 2000; Eickmann et al., 2009; Zhang et al., 2020). Along the spreading centers, hydrothermal fluids from the deep oceanic crust can move upwards through faults and escape at the ocean floor, resulting in a black smoker (Charlou et al., 2002) or a white smoker vent fluids (Kelley et al., 2001) that favour precipitation of carbonates (Turchyn et al., 2021) and dolomites (Roberts et al., 2013). Experimental investigation suggests that dolomitization can take place in marine and the lacustrine environments under low dissolved sulphate concentrations and silica diagenesis (Baker and Kastner, 1981). Geological models for dolomitization depend on the physicochemical conditions that can be produced in a range of environments in both eogenetic and mesogenetic settings (Braithwaite, 1991).

Base metal sulphide (pyrite, chalcopyrite, sphalerite, galena and other ore minerals) mineralization is ubiquitous in sedimentary basins and is common in rocks ranging in age from Paleoproterozoic (Wheatley et al., 1986; Deb et al., 1989; Pirajno and Joubert, 1993; Kesler and Reich, 2006) to Cenozoic (Megaw et al., 1988; Leach et al., 2001; Zhang et al., 2020). Proterozoic orogenic belts of the Pan-African age located between Congo and Kalahari cratons at the Otavi Mountain Land (Namibia) metallogenic province hich covers an area of approximately 10000 km^2 (Pirajno and Joubert, 1993). There are more than 600 carbonate-hosted base metal deposits in the sedimentary platform of the Damara Orogen affected by carbonate alteration evidenced in dolomite and calcite veins along with epigenetic, hydrothermal, replacement, and open space filling deposits (Chetty and Frimmel, 2000). Economically viable concentrations of base-metal deposits in the Silver mines area (Ireland) are confined to the Carboniferous sequence of the Irish Midlands (Banks et al., 2002). Zinc-lead deposits belong to extensively dolomitised horizons within the limestones, whereas sulphide minerals occur as open space-fillings as well as fine-grained massive, and

disseminated mineralisation (Reed and Wallace, 2004). Precambrian dolomite of the Aravalli Supergroup commonly hosts base metal minerals while other accompanying rocks are phyllite, greywacke, quartzite and conglomerate (Sachan, 1993). Economic lead-zinc deposits associated with the Precambrian dolomite rocks of the Zawar mineral belt occur in mineable quantity. The Alwar district has attracted researchers who have focused mainly on the structural settings and style of mineralisation (Singh, 1984; Khan et al., 2014; Sajeev et al., 2019; Srivastava and Prakash, 2020; Sahoo et al., 2022). In this study, we discuss the geochemical evolution of dolomites from theThanagazi Formation of the Mesoproterozoic Alwar Basin in relation to the sedimentaary environment, provenance and base metal content.

Geological Settings

The study area is located in the northern part of the Delhi Fold Belt (Delhi Supergroup) in the Aravalli Craton in Peninsular India (Fig. 1a). The Alwar basin constitutes the central part of the North Delhi Fold Belt (NDFB), which occurs as a narrow linear belt in the south and central Rajasthan and fans out over a wider zone in the north-eastern Rajasthan (Fig. 1b). This basin formed one such depocenter which was separated from Bayan in the east and Khetri basin in the west by Pre-Delhi basement complex (Fig. 1b). The Alwar basin of the Delhi Supergroup (Table 1a) is nearly 6000m thick package of volcanic and sedimentary rocks that comprise three groups (Raialo, Alwar, and Ajabgarh). The Raialo Group consists of a lower calcareous and an upper arenaceous sequence (viz., the Dogeta and the Tehla Formation, respectively) with marble, phyllite and schist best exposed in the northeastern sector around Dogeta, Gola-Ka-Bas, Kharar, Jhiri, Tilwarhi, Todi and Kho-Dariba (GSI, 2019).

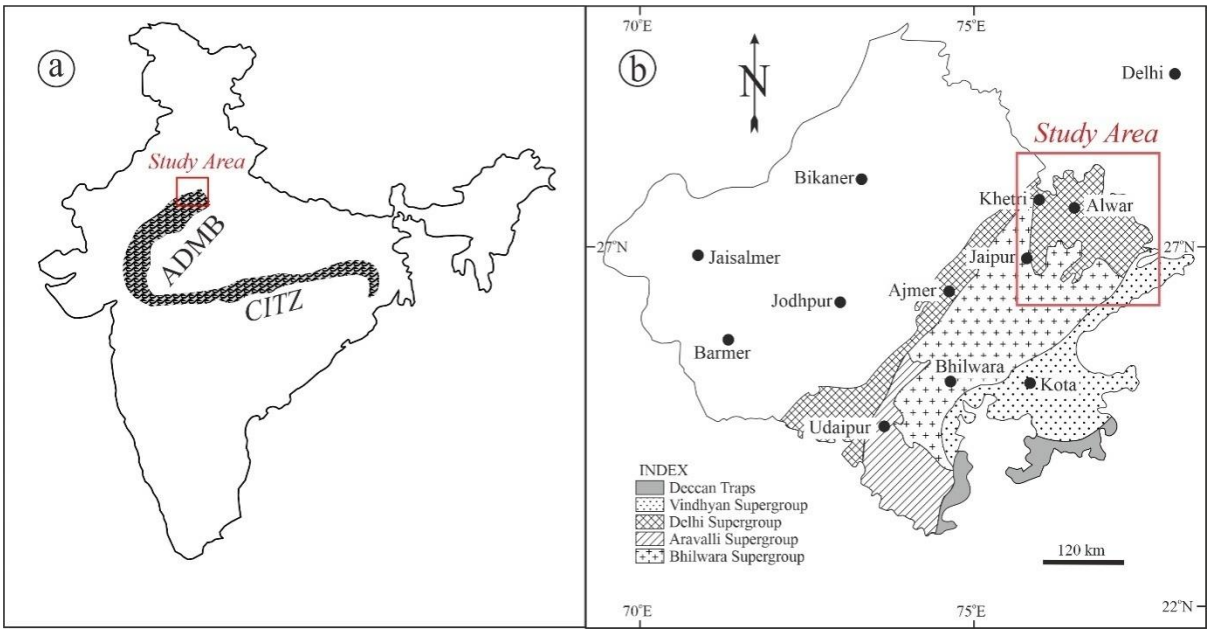

Fig. 1. (a) Location of the study area adjacent to the ADMB in the map of India; (b) outline of the geological map of Rajasthan shows the study area.

The Mesoproterozoic Alwar Group comprises metamorphosed arenaceous clastics with subordinate argillaceous and calcareous rocks interlayered with basic volcanics that rest unconformably over the Raialo Group (Table 1b). The generalized sequence of the Alwar Group is a basal conglomerate, arkose and quartzite followed by a sequence of argillaceous and impure calcareous rocks represented by pelitic schists which contain different mineral assemblages, impure marble and para-amphibolite which in turn is followed by a sequence of mainly arenaceous rocks with some amount of pelitic sediments (Fig. 1b). The rocks of the Mesoproterozoic Alwar Group have been classified into the Rajgarh, Kankawarhi, Pratapgarh, Nithar, Badalgarh, and Bayana Formation in northeastern Rajasthan and into the Srinagar and the Naulakha Formation in the Ajmer sector, respectively (GSI, 2001). The Mesoproterozoic Ajabgarh Group comprises of five formations (Table 1b). Metamorphosed argillites with intercalated arenites and subordinate carbonates have been included in the Kushalgarh and the Sariska formations. Carbonaceous phyllite, an interlayered sequence of quartzite, phyllite and schists containing chlorites, garnet, staurolite and andalusite are included under the Thanagazi, Bhakrol, and Arauli formations (GSI, 2019).

The Mundiyawas-Khera block located southwest of Thanagazi in the Mesoproterozoic Alwar Basin reveals a felsic volcanic-hosted thick copper and associated gold mineralization in the

Thanagazi Formation of Ajabgarh Group within the NDFB (Khan et al., 2014). The exposed rock types in the Mundiyawas-Khera area are meta-volcanosedimentary sequence, tremolite bearing dolomitic marble and carbonaceous phyllite (Fig. 2).

Table 1. (a) Stratigraphy of the Delhi Supergroup in the Alwar sub-basin (after Geological Survey of India, 2019).

Age	Supergroup	Group	Formation
Mezoproterozoic	Delhi Supergroup	Ajabgarh Group	Arauli Formation
			Bhakrol Formation
			Thanagazi Formation
			Seriska Formation
			Kushalgarh Formation
		Alwar Group	Pratapgarh Formation
			Kankwarhi Formation
			Rajgarh Formation
		Raialo Group	Tehla Formation
			Serrate Quartzite Formation
			Dogeta Formation

Table 1. (b) Lithostratigraphy of the Delhi Supergroup in the Alwar sub-basin (after Geological Survey of India, 2019).

Intrusives			Quartz vein and calcite vein
Delhi Supergroup (Mesoproterozoic)	Ajabgarh Group	Thanagazi Formation	Tremolite marble with quartzite
			Carbon phyllite
			Pyrite bearing biotite - quartzite
			Tremolite marble, biotite - marble
			Carbon phyllite/mica-schist/biotite marble
			Tremolite marble with quartzite
		Seriska Formation	Quartzite
		Kushalgarh Formation	Calcareous facies rocks – biotite – marble & dolomite – marble) hosting mineralization), calc. quartzite, calc. banded semipelite
	---------- Local Unconformity ----------		
	Alwar Group	Pratapgarh Formation	Tehal Formation
			Serrate Quartzite Formation
			Dogeta Formation
		Kankwarhi Formation	Conglomerate, mica schist, metavolcanics
	---------- Local Unconformity ----------		
	Raialo Group	Tehla Formation	Quartzite

Table 1. (c) Lithostratigraphy of Amra Ka Bas area in the Thanagazi Formation in the present study (after Geological Survey of India, 2019).

Meso-Proterozoic Age	Delhi Supergroup	Ajabgarh Group	Intrusive	Quartz vein
			Thanagazi Formation	Felsic metavolcanics
				Tremolite-bearing dolomitic marble
				Cherty quartzite
				Carbon phyllite

The felsic volcanics are represented by felsic tuff, lapilli tuff and agglomeratic tuff, which are rhyodacite in composition and occur as an interlayered sequence within the fine-grained quartzite, carbonaceous phyllite and dolomitic marble of Ajabgarh Group (Table 1c). The copper mineralization in Mundiyawas-Khera is hosted within the meta-volcanosedimentary sequence, dolomite, and tremolite-bearing dolomitic marble (Srivastava and Prakash, 2020). Sulphide ore minerals identified in this area as disseminations and stringers of pyrrhotite, pyrite and chalcopyrite which suggest base metal mineralization (Sajeev et al., 2019). Similar associations of sulphide ore minerals with volcanic rocks are also observed in various localities around Amra-Ka-Bas, Biharisar, Mejorh, Madri-Kishori, Bikrampura, etc.

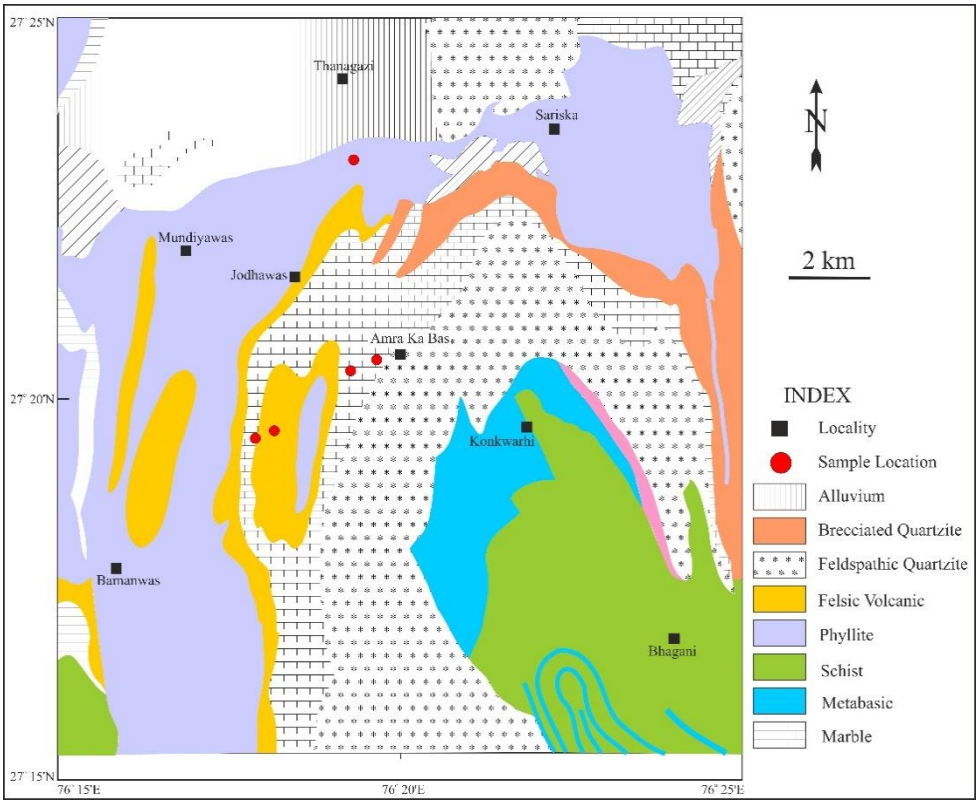

Fig. 2. Generalized local geological map of the Amra Ka Bas area in Thanagazi Formation with sample locations (Courtesy: Geological Survey of India).

Measured Litholog and Sampling Plan

Bulk dolomite samples are collected across the strike of the tremolitic marble interbanded with carbon phyllite. Litho-log of the study area around Amra Ka Bas and adjoining area is presented in the figure. Representative dolomite samples covering the stratigraphic lithosections were selected for bulk geochemical analysis using XRF and ICP-MS.

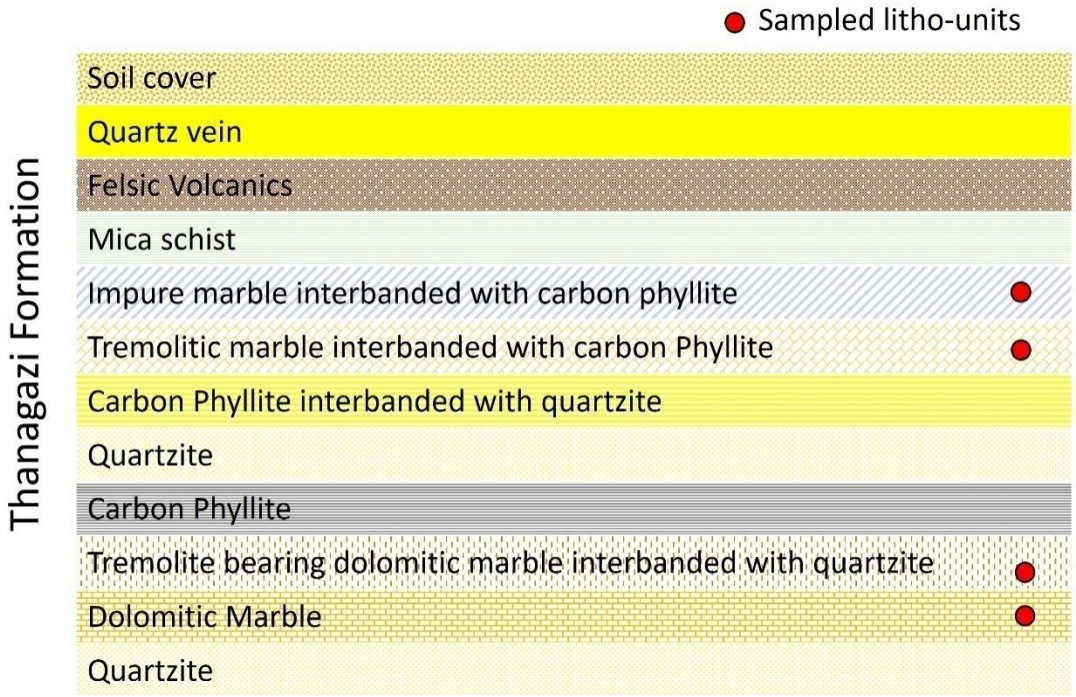

Figure: Detail lithological logs of Thanagazi Formation along Amra Ka Bas and adjoining area.

Lithological Associations

Dark grey coloured, very fine grained dolomite occurs along with dissolution cavities in the Amra Ka Bas area in association with volcano-sedimentary rocks (Fig. 3a). At some places, brown coloured carbonate matrix is also present in the dissolution cavities of dolomites. Micritic ferruginous dolomite occurs in few centimeters thick interbedded layers. Oxidation and ferruginisation of dolomite are also observed at several places around the Amra Ka Bas area (Fig. 3b). The buff grey coloured medium to fine grained crystalline dolomite shows profuse development of rosettes of tremolite. Occasional elephant skin weathering is observed on the surface of crystalline dolomite (Fig. 3c). The crystalline dolomite is brecciated due to silicification, shearing, grain rotation, and fragmentation. The crystalline dolomite is traversed by late-stage quartz veins which contain chalcopyrite and pyrrhotite grains along with malachite stains. The rotation of stretched and boudinaged quartz veins indicates simple shear stress in the dolomites of Amra Ka Bas area. It is intercalated with quartzite bands of variable thickness that range between 10-20 cm. Structural features like fold and boudinage are also present in the carbonate'smatrix at several places. White coloured material is coarsely crystalline calcite, which occurs as lining and partially fills small size cavities or vughs in dolomite (Fig. 3d). Tremolite occurs as broom shaped or slender type prismatic crystals of >5 cm size (Fig. 3e). In microphotograph, subhedral to euhedral prismatic crystals of tremolite shows distinct blue to green interference colours under cross polarized light (Fig. 3e, f). Most commonly, cracks and fissures are partially filled with calcite, quartz, and other secondary minerals in the dolomite are found in the Thanagazi Formation.

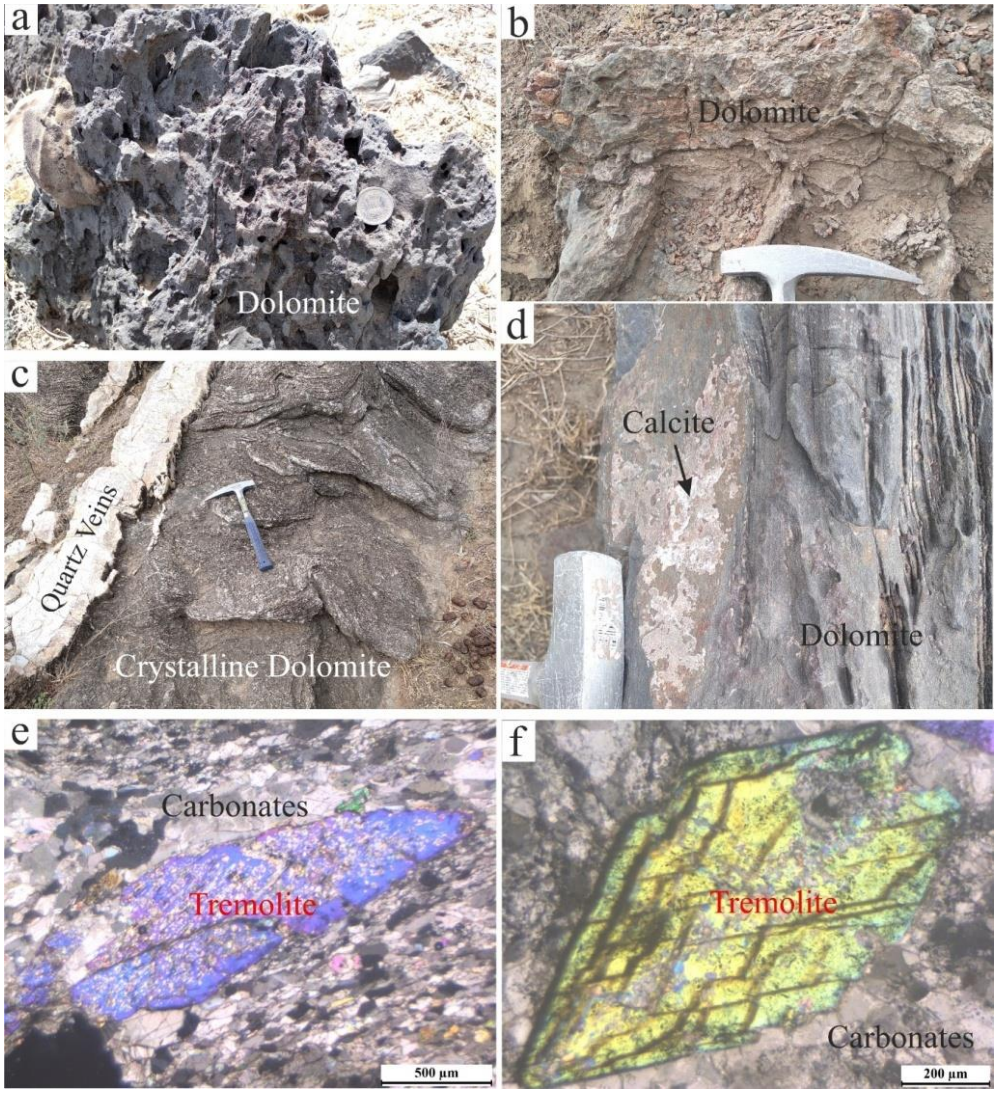

Fig.3. Field photographs of exposed dolomiteoutcrops near Amra Ka Bas area: (a) dissolution cavities and perforated surface of dolomite, (b) ferruginous intercalations with dolomite, (c) quartz veins in crystalline dolomite with elephant skin texture, and (d) bedded dolomite outcrop with calcite encrusts. Microphotographs of crystalline dolomite: (e) tremolite crystal in carbonate matrix and (f) euhedral tremolite grain with two sets of cleave planes in dolomite.

Analytical Methods

X-ray Fluorescence Spectrometer (XRF)

Representative rock samples, two kg each from dolomites were air-dried and fragmented to about 1 cm size and divided into 8 parts by coning and quartering. One part each (about 250 gm) was pulverized to -200 mesh size to a homogenous powder with the help of WC Planetary Mill. Care was taken at each stage of sample preparation such as crushing, coning-quartering, and pulverizing to avoid contamination. Six grams of each sample were powdered, thoroughly mixed with 0.6 gm of wax and poured into an aluminum cup. Homogenized samples were pressed at 40 tons using a hydraulic press to prepare pellets of 30 mm diameter and 5 mm thickness aluminum cup. These pellets were analyzed using a Bruker S8 Tiger wavelength dispersive X-ray fluorescence spectrometer (WD-XRF) having a 4 kW Rh anode X-ray target and operated at 30-50 KV and 50-100 mA. Several international rock, soil, and sediment standards (India, USGS, France, and China) were used for calibration (Singhal et al., 2019).

Inductively Coupled Plasma Mass Spectrometry (ICP-MS)

The homogenous powder rock samples were selected for the ICP-MS analysis in digested solution form, which essentially requires a very high quality, ultra-purified reagent, water and thoroughly cleaned crucibles and glassware. Millipore purified water (18 MΩ) was used in all investigations. PTFE Teflon beakers were used for open digestion of powdered rock samples where the teflon beakers and other glassware were cleaned with 1%HCl and millipore purified water. Analytical grade HF, analytical reagent (AR) grade $HClO_4$, distilled HNO_3 and HCl chemical reagents were used during the sample preparation. The sample preparation was done as follows: weight 0.05 g of -200 mesh size powdered rock sample with the help of electronic balance on butter paper, where the weighing is done up to four decimal points. For making the solution, 0.05 gm of each powdered rock sample was weighed, transferred weighed sample into ultra cleaned and thoroughly dried PTFE Teflon beakers and moistened with a few drops of ultra-pure water. 10 ml of an acid mixture of HF, HNO_3 and $HClO_4$ in the ratio of 7:3:1 were added to each sample in a Teflon beaker and swirled until the sample got completely moist. 1ml of 5 µg ml^{-1} of Rh solution was added to act as an internal standard in the beakers, it was covered with a lid and kept overnight for digestion. Next day, the beakers were heated on a hot plate at 200ºC after removing the lids in the fume hood chamber for about 1 hour, samples were allowed to evaporate until a crust or crystalline paste was obtained. The crust contents were dissolved in a beaker with 10 ml of 1:1 HNO_3 solution and kept on the hot plate for 10 minutes with moderate heat of ~70ºC. The sample was dissolved until all suspended particles came into the solution. The solution was made up to 250 ml volume with purified water in a cylindrical flask. The sample was kept in ultra-cleaned polythene sample bottles for analysis with proper labeling. All quantitative measurements were performed using instrument software Perkin Elmer SCIEX quantitative ELAN Version 3.4 software. Trace and rare earth element (REE) concentrations were analysed within accuracy ranges from 2 to 12% and precision varies between 3% to 8% by Inductively Coupled Plasma Mass spectrometry (ICP-MS, ELAN DRC-E, Perkin Elmer). ICP-MS instrumental parameters: RF power = 1100 W; Argon gas flow in (i) Nebuliser = 0.89 L/min, (ii) auxillary = 1.2 L/min, (iii) plasma 15 L/min; Lens voltage = 6V; sample uptake rate = 0.80 ml/min (Khanna et al., 2009). Acquisition parameters of ICP-MS: measuring mod – peak hopping; point per peak = 1; number of sweeps = 50; dwell time = 50 µs; integration time = 2500 ms; replicates = 3; internal standard = ^{103}Rh at an overall concentrations of 20 ng/ml. Japanese rock reference standards (JG-1a, JG-2) for granites were used to minimize the matrix effects. The acid-digested rock solutions were used in analyses where the sample introduction system in the instrument consists of a standard Meinhard nebulizer with a cyclonic spray chamber.

Geochemistry

The major and trace element composition of whole-rock samples are shown in tables 2 and 3. Sediment samples from the Amra Ka Bas were characterized by significant variations of the major component (Table 2). Major element geochemical composition of Amra Ka Bas samples plotted on the triangular diagram {$(Al, Fe)_2O_3.xH_2O$ – $(Ca,Mg)CO_3$ – SiO_2} of hydrated clays-carbonate-sand (Mason and Moore, 1982) are restricted to the dolomite field (Fig. 4a). At the same time, in the AKF {Al_2O_3 – (K_2O+Na_2O+CaO) – (Fe_2O_3+MgO)} ternary discrimination diagram (England and Jorgensen, 1973), these samples correspond to carbonaceous ferrite field (Fig. 4b).

Geochemistry of sediments normally reproduces the provenance of their source rocks (Roser and Korsch, 1986). The geochemical data of Amra Ka Bas sediments were compared with North American Shale Composite (NASC; data from Gromet et al., 1984) and Post Archean Australian Shale (PASS; data from Taylor and Mc Lennan, 1985). In the Al_2O_3 versus SiO_2 diagram (Barbera et al., 2006), they mainly resemble the trends of biogenic components whereas the detrital component is negligible (Fig. 5a). Binary discriminant diagram, MgO versus CaO (Siyi et al., 2019) displays mixed characteristics of the sedimentary and metasomatic line (Fig. 5b).

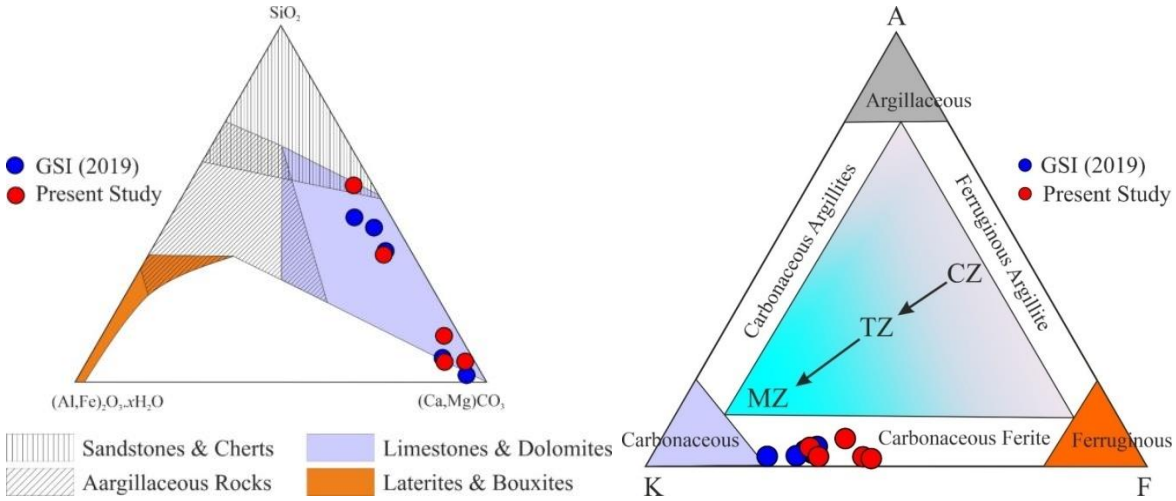

Fig.4. (a) Triangular diagram of hydrated clays [$(Al,Fe)_2O_3.xH_2O$] – carbonate [$(Ca,Mg)CO_3$] – Sand (SiO_2)displays the geochemical composition of sediments (afterMason and Moore, 1982), and (b) AKF Ternary discrimination diagram (after Englund and Jorgensen, 1973) of Al_2O_3 – (K_2O+Na_2O+CaO) – (Fe_2O_3+MgO) for representative samples of dolomites from Amra Ka Bas in Alwar basin.

Table 2. Bulk rock major oxides composition (wt%) of dolomite from Amra Ka Bas area in Alwar basin, Northwest India.

Rock Type	Crystalline Dolomite	Dolomite	Dolomite	Dolomite	Crystalline Dolomite
Sample No	59	64	AKB1	AKB24	31
SiO_2	27.67	42.27	3.15	3.06	7.16
Al_2O_3	1.59	1.83	0.56	0.54	0.31
TiO_2	0.1	0.1	0.045	0.042	0.042
Fe_2O_3	3.76	1.59	3.46	0.6	1.71
MnO	0.48	0.04	0.091	0.016	0.402
MgO	11.72	11.31	19.11	16.43	19.78
CaO	32.46	19.37	29.44	32.19	25.97
Na_2O	0.08	0.06	0.068	0.029	0.054
K_2O	0.25	0.61	0.14	0.54	0.34
P_2O_5	0.07	0.59	0.033	0.011	0.01
L.O.I.	21.78	20.51	42.76	42.38	47.07
Total	99.96	98.28	98.857	95.838	102.848
Ca/Mg	3.28	2.03	1.83	2.32	1.56
T(°C)	133	101	95	109	86

*Note: Temperature (T °C) of dolomite formation is estimated using the formulation of Rosenberg and Holland (1964).

For the recognition of the provenance sediments, it is important to depend on the least mobile geochemical elements during weathering, transport, diagenesis and metasomatism (Wronkiewicz and Condie, 1987). In the Fe_2O_3/Al_2O_3 vs $Al_2O_3/(Al_2O_3+Fe_2O_3)$ diagram (Murray, 1994; Girty et al., 1996), the Amra Ka Bas sediment samples plotted outside the area representing continental margin, pelagic, and ridge-proximals as well as old upper continental crust provenance subfields (Fig. 5c). All these depositional environments are independent of diagenetic modification intrinsic to dolomite chemistry (Murray, 1994). In the Fe_2O_3/TiO_2 vs $Al_2O_3/(Al_2O_3+Fe_2O_3+MnO)$ diagram (Bostrom, 1973), all sediment samples from Amra Ka Bas were plotted along the mixing curve of the two end-members of hydrothermal and argillite sources (Fig. 5d). On the whole, the mixed source for the dolomite precipitation around the Amra Ka Bas area is inferred from the geochemical investigations.

Table 3. Trace elements content (ppm) of dolomite from Amra Ka Bas area in Alwar basin, Northwest India.

Rock Type	Crystalline Dolomite	Dolomite	Dolomite	Dolomite	Crystalline Dolomite
Sample No	59	64	AKB1	AKB24	31
Ba	168.28	ND	30.04	61.04	15.07
Cr	ND	ND	ND	ND	ND
V	37.63	ND	5.7	17.91	19.3
Sc	2.15	0.8	1.53	1.47	2.58
Co	9.17	22.02	4.66	4.22	6.94
Ni	ND	ND	2.4	2.84	6.9
Cu	55.29	54.12	7.54	11.33	6.79
Zn	129.26	37.28	17.24	34.41	76.95
Ga	2.04	0.96	0.45	1.52	0.73
Pb	16.7	28.69	4.99	6.96	13.17
Th	1.38	1.62	0.8	0.98	0.69
Rb	3.58	11.8	3.12	10.43	9.58
U	1.53	1.6	1.47	0.66	1.01
Sr	33.52	33.57	53.12	55	53.41
Y	20.2	4.39	2.57	2.86	5.63
Zr	25.83	18.91	12.33	17.12	18
Nb	0.42	0.1	0.22	0.53	0.66

Rare Earth Elements Signature

Trace and rare earth element (REE) signatures of limestone and dolomites have been widely used to reconstruct the paleoenvironment of sedimentation (Frimmel, 2009; Franchi, 2018; Liu et al., 2019). It is also considred as reliable indicator of geochemical processes for the evolution of carbonate systems (Ozyurt et al., 2020). Redox-sensitive elements show diverse geochemical behaviour, which is mostly considered a natural proxy for revealing interaction processes between particles, solution, and redox reactions (Qing and Mountjoy, 1994; Li et al., 2019). These geochemical proxies are very supportive to rebuild early environmental settings (Sarangi et al., 2017; Mongelli et al., 2018). Geochemical analysis of REE in dolomite from the Amra Ka Bas area of Thanagazi Formation is presented in table 3.

The normalized pattern of the upper continental crust (UCC), spider diagram of dolomite samples from Amra Ka Bas shows Ba, U, P, and P enrichment, whereas, Th, Nb, and Ti show depletion trends (Fig. 6a). Enrichment of Ba is inversely related to the concentration of dissolved sulphate in the dolomitizing fluids (Di Bella et al., 2020). Inspite of this fact, it has been proposed that high salinity fluids yield high Sr content (1453 ppm; Lucia and Major, 1994; Hanor, 2004), whereas, mixing zone dolomites can be distinguished based on their low Sr content (Fouke and Reeder, 1992).

The normalized condition of the Post Archean Australian Shale (PAAS), dolomite samples from the Amra Ka Bas in Thanagazi Formation shows weakly depleted light rare earth elements (LREE) as compared to heavy rare earth elements (HREE) pattern (Fig. 6b). The abundance of Eu in the dolomite is related to the oxygen fugacity (fO_2), which means the reducing or oxidizing nature of the involved fluids (Di Bella et al., 2020). Geochemical stability of Eu^{3+} towards higher fO_2 and oxidation of Eu^{2+} under mildly acidic conditions improve to more oxidized environments (Bau, 1991; Kucera et al., 2009). Eu^{3+}/Eu^{2+} ratio is controlled by oxidation (Kamber and Webb, 2001; Zhang et al., 2014). According to Bau and Moller (1992), dolomite precipitation would involve Eu^{3+} ions, it would display a positive Eu anomaly due to the dispersion of the large Eu^{2+} ions from the dolomite crystal lattice.There is presence of a slightly positive anomaly of Eu displayed by some studied samples on the REE pattern (Fig. 6b) which suggests that environmental situations in which dolomite originated were to some extent oxidizing type.

Table 4. Rare earth elements content (ppm) of dolomite from Amra Ka Bas area in Alwar basin, Northwest India.

Rock Type	Crystalline Dolomite	Dolomite	Dolomite	Dolomite	Crystalline Dolomite
Sample No	59	64	AKB1	AKB24	31
La	5.396	3.635	3.328	2.327	2.442
Ce	10.847	7.018	6.208	4.358	5.32
Pr	1.971	0.973	0.711	0.54	0.722
Nd	6.412	3.701	3.579	2.816	4.642
Sm	2.178	0.864	0.494	0.359	0.895
Eu	0.484	0.234	0.087	0.202	0.335
Gd	2.875	0.867	0.459	0.332	0.796
Tb	0.51	0.125	0.07	0.049	0.135
Dy	3.17	0.684	0.456	0.353	0.886
Ho	0.642	0.131	0.106	0.089	0.214
Er	1.61	0.344	0.314	0.258	0.52
Tm	0.242	0.047	0.055	0.041	0.084
Yb	1.6	0.311	0.26	0.216	0.434
Lu	0.228	0.047	0.041	0.034	0.061

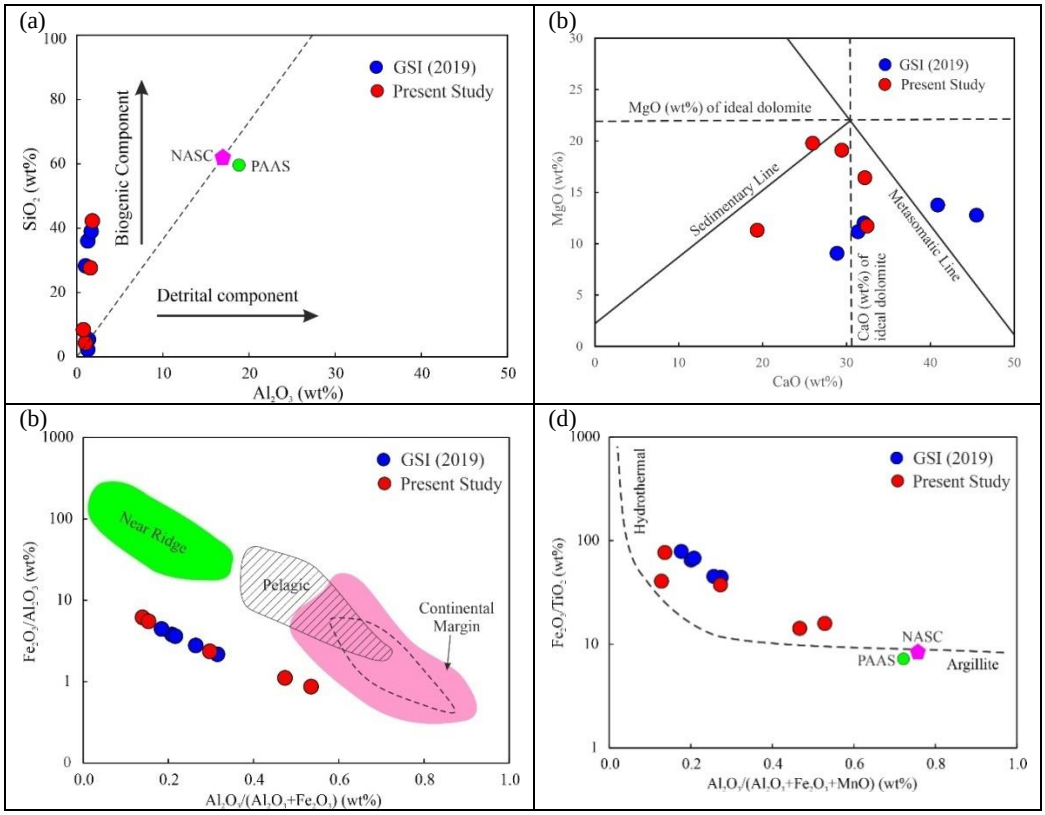

Fig.5. (a) Binary Al_2O_3 vs. SiO_2 diagram shows the presence of biogenic contribution in the present study, (b) Binary discrimination diagram MgO vs. CaO to distinguished dolomite forming processes (after Siyi et al., 2019), (c) Murray (1994) diagram displayed to discriminate depositional environment of sediments with old upper continental crust provenance subfield (dashed line-delimited area, after Girty et al., 1996), (d) Bostrom (1973) diagram shows end members mixing modelling curve of argillite and hydrothermal components with PAAS and NASC (data from Gromet et al., 1984; Taylor and McLennan, 1985), for representative samples of dolomites from Amra Ka Bas area in Alwar basin.

Base Metal Enrichment

The stability of dolomite in carbonate-rich hydrothermal solution indicates incongruent solubility towards low temperature whereas calcite field narrows towards higher temperature (Rosenberg and Holland, 1964). Dolomite precipitation in the sedimentary depositional environment is variable in composition within the temperature range between 25 to 200ºC (Arvidson and Mackenzie, 1999; Jiang et al., 2016; Banerjee, 2016). Experimental investigation demonstrated that the Ca/Mg ratio is directly proportional to the temperature of hydrothermal solutions up to 420ºC in the thermodynamic stability limit of calcite, dolomite and magnesite (Rosenberg et al., 1967). In the present study, the temperature of dolomite formation is calculated using the formulation of Rosenberg and Holland (1964). The calculated temperature of dolomite formation for the Amra Ka Bas samples ranges from 86-133ºC which is dependent on the Ca/Mg ratio (Table 2). Geochemical data reported by the Geological Survey of India (2019) has also been used to estimate the temperature of dolomite formation, which ranges from 130-152ºC.

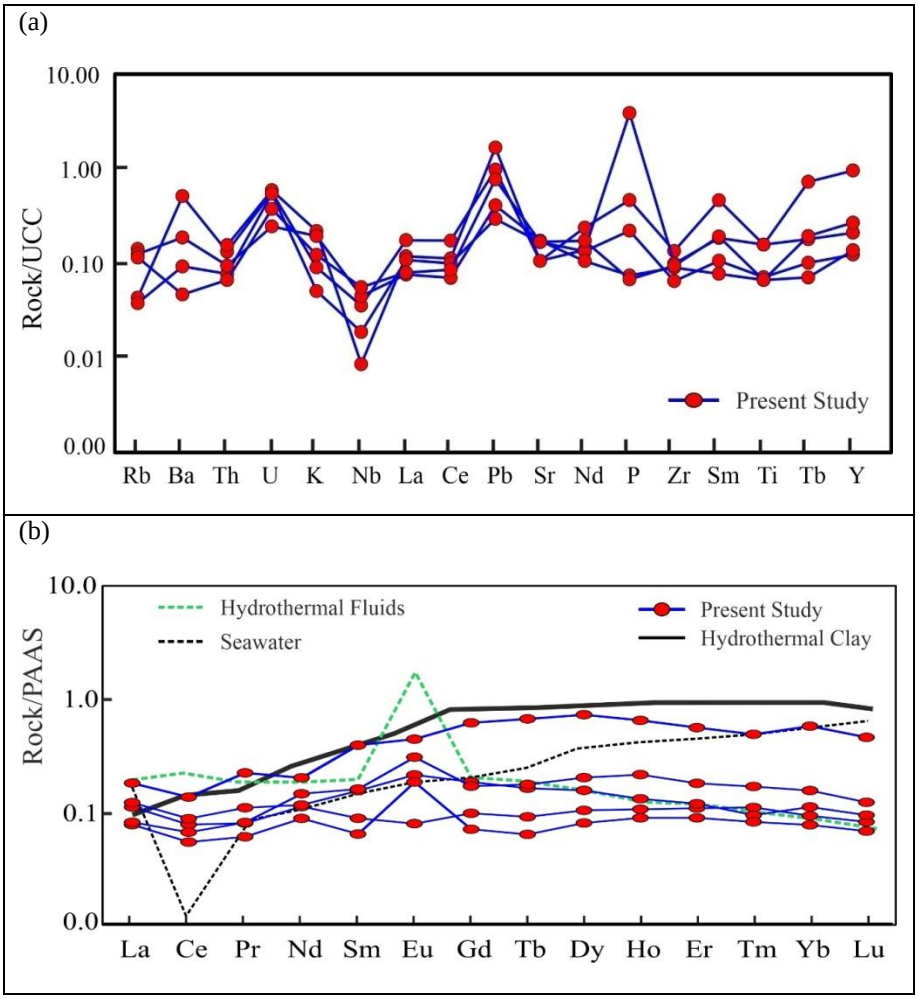

Fig.6. (a) Upper continental crust (UCC) normalized spider diagrams and (b) PAAS normalized REE patterns for representative samples of dolomites from Amra Ka Bas in Alwar basin. REE chemistry of seawater (Surya Prakash et al., 2012), hydrothermal fluids and clay (Severnmann et al., 2004), UCC(Rudnick and Gao (2003),and PAAS(Taylor and McLean, 1985) are taken from earlier studies.

Solubility of base metal in the hydrothermal fluid strongly depends on the temperature (Skinner, 1979; Pirajno, 1992; Zotov et al., 1994; Wood and Samson, 1998; Seward et al., 2014). Temperature versus copper concentration diagrams (Fig. 7a) indicate that hydrothermal fluids derived from different sources (black and white smokers) may have aplausible mechanism to enrich dolomite. Dissolved zinc concentration in hydrothermal fluids accelerates dolomite formation in shallow marine conditions (Vandeginste et al., 2019). Most of the marine hydrothermal vent fluids show high zinc concentration (<400 ppm) in the temperature range of 200 to 400ºC whereas zinc content in dolomite from Amra Ka Bas signifies a different scenario (Fig. 7b). Low temperature (100ºC) hydrothermal fluid associated with organic carbonate component related to the diagenetic processes in sedimentary basin

favour zinc enrichment in dolomite (Giordano, 2002).Thus, it could be inferred that there was a significant enrichment of zinc during the dolomite formation in the Amra Ka Bas possibly derived from a low-temperature hydrothermal fluid source during the diagenetic processes.

High-temperature hydrothermal vent fluids have been identified as the major source of base metal accumulation in the mid-ocean ridges, arc, and backarc spreading centers, mostly emitted from black and white smoker type plumes (Hannington et al., 2011; Edmond et al., 1995; Von Damm et al., 2003; Diehl and Bach, 2020). The chemical composition of seawater is quite different from the hydrothermal vent fluid that discharges from the ocean bottom at mid-ocean ridges and sea mounts (Corliss et al., 1979; Edmond et al., 1982). The composition of the dissolved material in the hydrothermal vent fluids is similar to the chemistry of hydrothermal particulate phases and appears to act as a significant source of dissolved base metals contents (German et al., 1991).

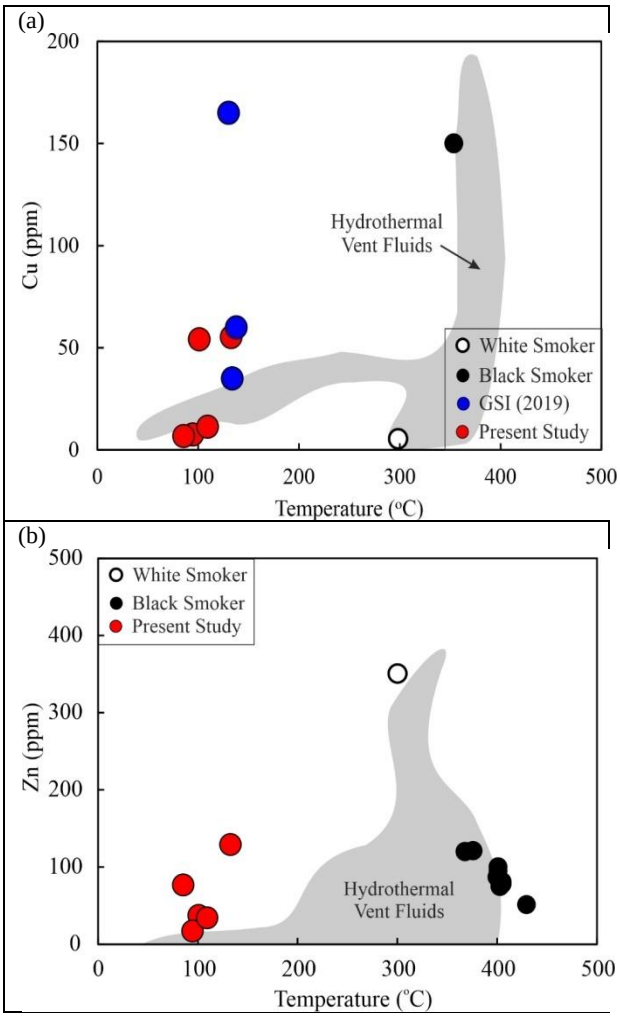

Fig.7. (a) Temperature versus copper solubility and (b) temperature versus zinc solubility in the hydrothermal system (after Rosenberg and Holland, 1964). Data for the composition of hydrothermal vent fluid (Diehl and Bach, 2020), black, and white smokers (Edmond et al., 1995; Von Damm et al., 2003) are taken from published literature.

A comparison of base metal concentrations (Cu and Zn) within the hydrothermal vent fluids and dolomite samples of the Amra Ka Bas area reveals their geochemical similarity, which may be derived from sources possibly of black smoker types (Fig 8a). In shallow subseafloor settings, thermal alteration of organic carbon and mudstones are considered to be the most significant factors for the enrichment of high concentrations of base metals (Pb, Zn) into the particulate phases of deposition (Magnall et al., 2016). The concentration of Pb in the dolomite samples is relatively low as compared to the chemistry of hydrothermal vent fluid (Fig. 8b) which indicates that the Pb scavenges were from other sources and contributed to the dolomitizing fluids in the area of investigation. Thus, it can be inferred that the mixing of hydrothermal fluids from two different sources possibly occurred during the dolomitization in the Amra Ka Bas area in the shallow subseafloor settings or marine conditions.

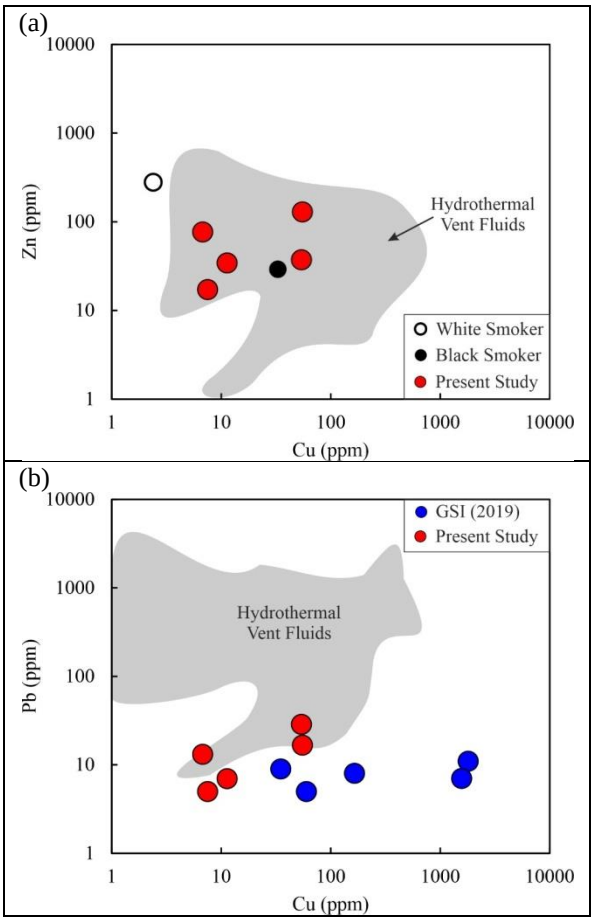

Fig.8.(a) Cu vs. Zn (ppm) and (b) Cu vs. Pb (ppm) content in the hydrothermal system. Data for the composition of hydrothermal vent fluid (Diehl and Bach, 2020), black, and white smokers (Edmond et al., 1995; Von Damm et al., 2003) are taken from published literature.

Discussions

Dolomite occurrences in the Amra Ka Bas area are supported by field observations of fine grained (amorphous) and coarse grained (crystalline)

dolomites. Generally, amorphous type dolomite is characterized by micritic-aphanitic textures, and laminated structures, and is a little porous (Fig 3a,b). Fine-grained dolomite precipitation may be connected to the synsedimentary hydrothermal fluid circulation in the sedimentary basin (Wen et al., 2007; Zhang et al., 2020). Crystalline dolomite (Fig. 3c) in the area shows coarse to very coarse grained clastic texture with shapes from sub-euhedral (xenotropic texture) to euhedral (idiotopic texture) with internal cavities along with pore-spaces (Gregg and Sibley, 1984). Interpretation of geochemical data of dolomite suggests a multistage evolution of dolomite in the area of investigation. The origin of crystalline dolomite can be attributed to the basin evolution, since dolomitization may take place at the diagenetic stages (Di Bella et al., 2020). Digenetic dolomitization coupled with the action of burial while the dolomitizing fluids transformed the slightly porous dolomites into nonporous mosaic dolomite (Montanez, 1997). The grain size of dolomite suggests the sedimentary environmental conditions in which the dolomitization occurs are evaporitic (Behrens and Land, 1972) or mixing water (Hanshaw et al., 1971) or marine type (Land, 1985). Evaporitic dolomite is associated with gypsum-anhydrite mineral and commonly occurs in a supra-tidal environment characterized by excessive evaporation under continental climatic conditions (Goldberg, 1967). Mixing water (seawater and freshwater) explains the formation of dolomite in the platform margin sections through the interaction of sea-level fluctuations, sedimentation, and subsidence (Badiozamani, 1973; Humphrey and Quinn, 1989). Marine solutions can be the only source of a large amount of Mg^{2+} ions needed for dolomitization of massive platform dolomite possibly formed directly from seawater (Varol and Magaritz, 1992). The formation temperature of the amorphous dolomite was higher than those of the crystalline dolomite in the Amra Ka Bas area of theThanagazi Formation.

Chemical and biochemical sedimentary rocks are dominated by components that have been transported as ions in solution and are very susceptible to changes in composition and mineralogy during the diagenesis (Bridge and Demicco, 2012). In the present study, the biogenic contribution is strongly influenced the dolomitization processes in the Amra Ka Bas area. Environmental conditions were probably responsible for the varying relative contribution of the material available in controlling the composition of the sediments (Lihou et al., 1996; Pandey et al., 2019).

Various factors contribute to explain the geochemical variations in the dolomite from the Amra Ka Bas area. Integrated approach of geochemistry (major, trace and rare earth elements) of dolomitic rocks gives support to reveal the source area composition. Weathering actions of sedimentary rocks may be appraised through investigation of the associations among alkali and alkaline earth elements (Nesbitt and Young, 1984). Chemical alteration largely involves calcium, sodium and potassium, which are preferentially mobilised, whereas aluminium remains immobile (Ding et al., 2016). The process of determining the provenance and origin of sedimentary rocks is very useful in understanding the past events of geological processes, which may describe the evolution of the sediment from source to the basin of deposition (Haughton et al., 1991). Dolomites of the Amra Ka Bas area are mainly plotted in the sedimentary provenance field. Investigations on sediment provenance concerning the origin, composition, transportation, and deposition are an important part of understanding the links between basinal sedimentation and tectonics (Smyth et al., 2014).

Experimental investigation demonstrated that dolomite formation is affected by the temperature of the mineralogical reaction as the Ca/Mg ratio of the solutions increases up to 420ºC (Rosenberg and Holland, 1964; Sibley et al., 1987). Dolomite formation can be facilitated by precipitation, diagenesis, hydrothermal processes and metamorphism under a variety of conditions in marine and lacustrine environments (Baker and Kastner, 1981). It may be produced from seawater, continental waters, mixing of basinal brines, mixing of hypersaline brine with seawater or mixing of seawater with meteoric water or hydrothermal vent fluids (Warren, 2000). Several studies have reported the precipitation of penecontemporaneous dolomite from normal seawater or pore water (Saller, 1984; Mitchell et al., 1987; Lumsden, 1988) in subtidal to deep-sea environmental settings. Dolomite formation during geothermal convections promotes calcium-rich and magnesium-poor fluids in the carbonate platforms in the temperature range of 25 to 200ºC (Pokrovsky and Schott, 2001; Wilson et al., 2001; Banerjee, 2016). In the present study, geothermometric estimates obtained for the composition of dolomites from Amra Ka Bas indicate low temperature (86-152ºC) stability conditions, which is suitable for thermochemical sulphate reduction and the precipitation of base metals. Hydrothermal fluids commonly precipitate base metal sulphides (chalcopyrite, sphalerite, galena, etc.) and associated carbonate minerals (calcite and dolomite) in the temperature range of 60 to 250ºC (Gregg, 2004). Copper and zinc content of the Amra Ka Bas dolomites is similar to that of high-temperature vent fluids. However, Pb content in the dolomite suggests its origin from a relatively low-temperature fluid. Therefore, it can be inferred that the mixing of hydrothermal fluids from two different sources possibly of variable composition and temperature were responsible for dolomitization in the Amra Ka Bas area of the Thanagazi Formation.

Conclusions

Integrated lithological, geochemical and geothermometric investigation of dolomites from the Amra Ka Bas area suggest the involvement of weathering, transport and diagenesis in ultimate rock composition and provide an understanding of the source rock composition. The abundance of major and trace elements is considered mainly related to the source rock composition, which was controled by a provenance of the shallow marine sedimentary environment. The source area for the studied dolomite is identifiable with the mixing of hydrothermal and argillite constituents and is dominated by biogenic processes during the digenesis. Digenetic processes control the formation of dolomite in the area of study with significant enrichment of base metal concentration during the precipitation in the temperature range of 86-152ºC. Base metal content and temperature of dolomite formation suggest two possible sources of low and high temperature sediments which contribute to the dolomitization processes in the Thanagazi Formation of the Mesoproterozoic Alwar Basin.

Acknowledgements

We thank to the Head, Department of Geology, Institute of Science, Banaras Hindu University and Additional Director General, Geological Survey of India, Western Region for providing all the necessary facilities. DP acknowledges financial support from BHU IoE SEED Grant No 21185 (Dev. Scheme No. 6031). Thanks are due to Dr. A. K. Singh for XRF and ICP-MS facilities at Wadia Institute of Himalayan Geology, Dehradun, India.

References

Alderman, A.R., and vonderBorch, C.C. (1963), A dolomite reaction series. Nature, v. 198, p. 466-467.

Arvidson, R.S., and Mackenzie, F.T. (1999), The dolomite problem: control of precipitation kinetics by temperature and saturation state. American Journal of Science, v. 299, p. 257-288.

Badiozamani, K. (1973), The Dorag dolomitization model – application to the middle Ordovician of Wisconsi. Journal of Sedimentary Petrology, v. 43, p. 965-984

Baithwaite, C.J.R. (1991), Dolomites, a review of origins, geometry and textures. Transactions of the Royal Society of Edinburgh: Earth Sciences, v. 82, p. 99 – 112.

Baker, P.A., and Kastner, M. (1981), Constraints on the formation of sedimentary dolomite. Science, v. 213, p. 214-216.

Banerjee, A. (2016), Estimation of dolomite formation: dolomite precipitation and dolomitization. Journal of Geological Society of India, v. 87, p. 561-572.

Banks, D.A., Boyce, A.J., and Samson, I.M. (2002), Constraints on the origins of fluids forming Irish Zn-Pb-Ba deposits: evidence from the composition of fluid inclusions. Economic Geology, v. 97, p. 471-480.

Barbera, G., Mazzoleni, P., Critelli, S., Pappalardo, A., Giudice, A.L., and Cirrincione, R. (2006), Provenance of shales and sedimentary history of the Monte Soro Unit, Sicily. Periodico di Mineralogia, v. 75, p. 313-330.

Bau, M. (1991), Rare-earth element mobility during hydrothermal and metamorphic fluid–rock interaction and the significance of the oxidation state of europium. Chemical Geology, v. 93, p. 219–230.

Bau, M., and Möller, P. (1992), Rare earth element fractionation in metamorphogenic hydrothermal calcite, magnesite and siderite. Mineralogy and Petrology, v. 45, p. 231–246.

Behrens, E.W., and Land, L.S. (1972), Subtidal Holocene dolomite, Baffin Bay, Texas. Journal of Sedimentary Petrology, v. 42, p. 155–161.

Boni, M., Parente, G., Bechstädt, T., De Vivo, B., and Iannace, A. (2000), Hydrothermal dolomites in SW Sardinia (Italy): evidence for a widespread late-Variscan fluid flow event. Sedimentary Geology, v. 131, p. 181–200. doi:10.1016/s0037-0738(99)00131-1.

Bostrom, K., (1973), The origin and fate of ferromanganoan active ridge sediments. Stockholm Contribution in Geology, v. 27, p. 149-243.

Bouton, A., Vennin, E., Amiotte-Suchet, P., Thomazo, C., Sizun, J.P., Virgone, A., Gaucher, E.C., and Visscher, P.T. (2020), Prediction of the calcium carbonate budget in a sedimentary basin: A "source-to-sink" approach applied to Great Salt Lake, Utah, USA. Basin Research, v. 32, p. 1005-1034. doi: 10.1111/bre.12412.

Bridge, J.S., and Demicco, R.V. (2012), Earth Surface Processes, Landforms and Sediment Deposits. Cambridge University Press, Cambridge, p. 1-883.

Charlou, J.J., Donval, J.P., Fouquet, Y., Jean-Baptiste, P., and Holm, N. (2002), Geochemistry of high H_2 and CH_4 vent fluids issuing from ultramafic rocks at the Rainbow hydrothermal field (36º14'N, MAR). Chemical Geology, v. 191, 345-359.

Chetty, D., and Frimmel, H.E., (2000), The role of evaporites in the genesis of base metal sulphide mineralisation in the Northern Platform of the Pan-African Damara Belt, Namibia: geochemical and fluid inclusion evidence from carbonate wall rock alteration. Mineralium Deposita, v. 35, p. 364-376.

Corliss, J.B., Dymond, J., Gordon, L.I., Edmond, J.M., von Herzen, R.P., Ballard, R.D., Green, K., Williams, D., Bainbridge, A., Crane, K., and van Andel, T.H. (1979), Submarine thermal springs on the Galapagos rift. Science, v. 203, p. 1073-1083.

Deb, M., Thorpe, R.I., Cumming, G., and Wegner, P.A. (1989), Age, source and stratigraphic implications of lead isotope data for conformable sediment-hosted base metal deposits in Proterozoic Aravalli–Delhi orogenic belt, NW India. Precambrian Research, v. 42, p. 1–22.

Di Bella, M., Italiano, F., Romano, D., Quartieri, S., Pino, P., Tripodo, A., and Sabatino, G. (2020), Massive dolomites in the Messinian evaporitic sequence (Sicily,

Italy): multi-analytical characterization and implication for the dolomitization processes. Carbonates and Evaporites, v. 35, 29. https://doi.org/10.1007/s13146-020-00559-8.

Diehl, A. and Bach, W. (2020), MARHYS (MARineHYdrothermal Solutions) Database: A global compilation of marine hydrothermal vent fluid, end member, and seawater compositions," Geochemistry, Geophysics, Geosystems, v. 21, e2020GC009385. https://doi.org/10.1029/2020GC009385

Ding, K., Seyfried Jr., W.E., Tivey, M.K., and Bradley, A. M. (2016), In situ measurement of dissolved H_2 and H_2S in high-temperature hydrothermal vent fluids at the Main Endeavour Field, Juan de Fuca Ridge. Earth and Planetary Science Letters, v. 186, p. 417-425.

Edmond, J.M., Campbell, A.C., Palmer, M.R., Klinkhammer, G.P., German, C.R., Edmonds, H.N., Elderfield, H., Thompson, G., and Rona, P. (1995), Time series studies of vent fluids from the TAG and MARK sites (1986, 1990) Mid-Atlantic Ridge: a new solution chemistry model and mechanism for Cu/Zn zonation in massive sulphide orebodies, Hydrothermal Vents and Processes. In: Parson, L.M., Walker, C.L., and Dixon, D.R. (ed.), Geological Society London Special Publication, v. 87, p. 77–86.

Edmond, J.M., Von Damm, K.L., McDuff, R.E., and Measures, C.I. (1982), Chemistry of hot springs on the East Pacific Rise and their effluent dispersal. Nature, v. 297, p. 197-191.

Eickmann, B., Bach, W., Rosner, M., and Peckmann, J. (2009), Geochemical constraints on the modes of carbonate precipitation in peridotites from the Logatchev Hydrothermal Vent Field and Gakkel Ridge. Chemical Geology, v. 268, p. 97-106.

Englund, J.O. and Jorgensen, P. (1973), A chemical classification system for argillaceous sediments and factors affecting their composition. GeologiskaFöreningeni Stockholm Förhandlingar, v. 95, p. 87-97.

Eriksson, K.A., and Warren, J.K. (1983), A paleohydrologic model for early Proterozoic dolomitization and silicification. Precambrian Research, v. 21, p. 299-321.

Fouke, B.W., and Reeder, R.J. (2018), Surface structural controls on dolomite composition: evidence from compositional sector zoning. Geochimica et Cosmochimica Acta, v. 56, p. 4015–4024.

Franchi, F. (2018), Petrographic and Geochemical Characterization of the Lower Transvaal Supergroup Stromatolitic Dolostones (Kanye Basin, Botswana). Precambrian Research, v. 310, p. 93-113.

Frimmel, H.E. (2009), Trace element distribution in Neoproterozoic carbonates as palaeoenvironmental indicator. Chemical Geology, v. 258, p. 338-353.

Geological Survey of India (2001) Geology and mineral resources of Rajasthan. Geological Survey of India, Miscellaneous Publication, v. 30(12), p. 1-113.

Geological Survey of India (2019), Copper-gold mineralization in Khera main block, Mundiyawas-Khera area, Alwar basin, Rajasthan: a prospective model for exploration. Bulletin Series A, v. 70, p. 1-160.

German, C.R., Campbell, A.C., and Edmond, J.M. (1991), Hydrothermal scavenging at the Mid-Atlantic Ridge: modification of the trace element dissolved fluxes. Earth and Planetary Science Letters, v. 107, p. 101-114.

Giordano, T.H. (2002), Transport of Pb and Zn by carboxylate complexes in basinal ore fluids and related petroleum-field brines at 100 ^oC: the influence of pH and oxygen fugacity. Geochemical Transactions, v. 3, p. 56-72.

Girty, G.H., Ridge, D.L., Knaack, C., Johnson, D., and Al-Riyami, R.K. (1996), Provenance and depositional setting of Paleozoic Chert and Argillite, Sierra Nevada, California. Journal of Sedimentary Research, v. 66, p. 107-118.

Goldberg, M. (1967), Supratidal dolomitization and dedolomitization in Jurassic rocks of HamakhteshHaqatan, Israel. Journal of Sedimentary Petrology, v. 37, p. 760-773.

Gregg, J.M. (2004), Basin fluid flow, base-metal sulphide mineralization and the development of dolomite petroleum reservoirs. Geological Society of London Special Publications, v. 235, p. 157-175.

Gregg, J.M., and Sibley, D.F. (1984), Epigenetic dolomitization and the origin of xenotopic dolomite texture. Journal of Sedimentary Petrology, v. 54, p. 908-931.

Gromet, L.P., Dymek, R.F., Haskin, L.A., and Korotev, R.L. (1984), The 'North American shale composite': its compilation, major and trace elements characteristics. Geochimica et Cosmochimica Acta, v. 48, p. 2469-2482.

Hannington, M., Jamieson, J., Monecke, T., Petersen, S., and Beaulieu, S. (2011), The abundance of seafloor massive sulfide deposits. Geology, v. 39, p. 1155-1158.

Hanor, J.S. (2004), A model for the origin of large carbonate- and evaporite-hosted celestine ($SrSO_4$) deposits. Journal of Sedimentary Research, v. 74, p. 168–175.

Hanshaw, B.B., Back, W., and Deike, R.G. (1971), A geochemical hypothesis for dolomitization by groundwater. Economic Geology, v. 66, p. 710–724.

Hardie, L.A. (1987), Dolomitization: a critical view of some current views. Journal of Sedimentary Petrology, v. 57, p. 166-183.

Haughton, P.D.W., Todd, S.P., and Morton, A.C., (1991), Development in sedimentary provenance studies. Geological Society London Special Publication, v. 57, p. 1-11.

Humphrey, J.D., and Quinn, T.M. (1989), Coastal mixing zone dolomite, forward modelling, and massive dolomitization of platform-margin carbonates. Journal of Sedimentary Petrology, v. 59, p. 438-454.

Jiang, L., Cai, C., Worden, R.H., Srowley, S.F., Jia, L., Zhang, K., and Duncan, I.J. (2016), Multiphase dolomitization of deeply buried Cambrian petroleum reservoirs, Tarim Basin, north-west China. Sedimentology, v. 63, p. 2130-2157.

Kamber, B.S., and Webb, G.E. (2001) The geochemistry of late Archaean microbial carbonate: Implications for ocean chemistry and continental erosion history. Geochimica et Cosmochimica Acta, v. 65, p. 2509–2525.

Kelley, D.S., Karson, J.A., Blackman, D.K., FruÈh-Green, G.L., Butterfield, D.A., Lilley, M.D., Olson, E.J., Schrenk, M.O., Roe, K.K., Lebon, G.T., and Rivizzigno, P. (2001), An off-axis hydrothermal vent field near the Mid-Atlantic Ridge at 30°N. Nature, v. 412, 145-149.

Kesler, S.E., and Reich, M.H. (2006), Precambrian Mississippi Valley-Type deposits; relation to changes in composition of the hydrosphere and atmosphere, In: Kesler S.E., and H. Ohmoto, H. (ed.), Evolution of early Earth's atmosphere, hydrosphere, and biosphere; constraints from ore deposits. Geological Society of America Memoirs, v. 198, p. 185–204.

Khan, I., Sahoo, P.R., and Rai, D.K. (2014), Proterozoic felsic volcanics in Alwar basin of North Delhi Fold Belt, Rajasthan: implication for copper mineralization. Current Science, v. 106, p. 27-28.

Khanna, P.P., Saini, N.K., Mukherjee, P.K., and Purohit, K.K. (2009), An appraisal of ICP-MS technique for determination of REEs: long term QC assessment of silicate rock analysis. Himalayan Geology, v. 30, p. 95-99.

Kucera, J., Cempirek, J., Dolnicek, Z., Muchez, P., and Prochaska, W. (2009) Rare earth elements and yttrium geochemistry of dolomite from post-Variscan vein-type mineralization of the NízkýJeseník and Upper Silesian Basins, Czech Republic. Journal of Geochemical Exploration, v. 103, p. 69–79.

Land, L.S. (1985), The origin of massive dolomite. Journal of Geoscience Education, v. 33, p. 112–125.

Leach, D.L., Taylor, R.D., Fey, D.L., Diehl, S.F., and R. W. Saltus, R.W. (2001), A deposit model for Mississippi Valley-Type lead-zinc ores. Scientific Investigations Report 2010-5070-A, U. S. Geological Survey, https://doi.org/10.3133/sir20105070A.

Lee, M.R., and Lindgren, P. (2015), 4.6-billion-year-old aragonite and its implications for understanding the geological record of Ca-carbonate. Carbonates and Evaporites, v. 30, p. 477–481.

Li, J., Redfern, S.A.T., and Giovannelli, D., (2019), Deep carbon cycle through five reactions. American Mineralogist, v. 104, p. 465–467.

Lihou, J.C., and Mange-Rajetzky, M.A. (1996), Provenance of the Sardona Flysch, eastern Swiss Alps: example of high-resolution heavy mineral analysis applied to an ultrastable assemblage. Sedimentary Geology, v. 105, p. 141-157.

Liu, J., Guo, H., Pourret, O., Wang, Z., Sun, Z., Zhang, W., and Liu, M. (2021), Distribution of rare earth elements in sediments of the North China Plain: A probe of sedimentation process. Applied Geochemistry, v. 134, 105089. https://doi.org/10.1016/j.apgeochem.2021.105089.

Liu, J., Song, J., Yuan, H., Li, X., Li, N., and Duan, L. (2019), Rare earth element and yttrium geochemistry in sinking particles and sediments of the Jiaozhou Bay, North China: potential proxy assessment for sediment resuspension. Marine Pollution Bulletin, v. 144, p. 79-91.

Lucia, F.J., and Major, R.P. (1994), Porosity Evolution through Hypersaline Reflux Dolomitization Ed. by B. Purser, M. Tucker, and D. Zenger (Dolomites). International Association of Sedimentologists Special Publication, v. 21, p. 345– 360.

Lumsden, D.N. (1988), Characteristics of deep-marine dolomite. Journal of Sedimentary Petrology, v. 58, p. 1023-1031.

Machel, H.G. (2004), Concepts and models of dolomitization: a critical reappraisal. In: Braithwaite, C.J.R., Rizzi, G., and Darke, G. (ed.), The Geometry and Petrogenesis of Dolomite Hydrocarbon Reservoirs. Geological Society of London Special Publication, v. 235, p. 7-63.

Magnall, J.M., Gleeson, S.A., Blamey, N.J.F., Paradis, S., and Luo, Y. (2016), The thermal and chemical evolution of hydrothermal vent fluids in shale hosted massive sulphide (SHMS) systems from the MacMillan Pass district (Yukon, Canada). Geochimica et Cosmochimica Acta, v. 193, p. 251-273.

Mason, B. and Moore, C.B. (1982), Principles of Geochemistry. John Wiley & Sons, Canada, p. 1-340.

McLennan, S.M., Hemming, S., McDaniel, D.K., and Hanson, G.H. (1993), Geochemical approaches to sedimentation provenance and tectonics. In: Johnsson M.J., and Basu, A. (ed.), Processes Controlling the Composition of Clastic Sediments. Special Paper of the Geological Society of America, v. 284, p. 21-40.

Megaw, P.K.M., Ruiz, J., and Titley, S.R. (1988), High-temperature, carbonate-hosted Ag-Pb-Zn(Cu) deposits of northern Mexico. Economic Geology, v. 83, p. 1856–1885.

Mitchell, J.T., Land, L.S., and Miser, D.E. (1987), Modern marine dolomite cement in a north Jamaican fringing reef. Geology, v. 15, p. 557-560.

Mongelli, G., Sinisi, R., and Paternoster, M., and Perri, F. (2018), REEs and U distribution in P-rich nodules from Gelasian Apulian Tethyan carbonate: A genetic record. Journal of Geochemical Exploration, v. 194, p. 19-28.

Montañez, I.P. (1997) Secondary porosity and late diagenetic cements of the upper Knox group, Central Tennessee region: a temporal and spatial history of fluid flow conduit development within the Knox regional aquifer. In: Montañez, I.P., Gregg, J.M., and Shelton, L.K. (ed.), Basin-Wide Diagenetic Patterns, v. 57, 101–117.

Murray, R.W. (1994), Chemical criteria to identify depositional environments of chert: general principles and applications. Sedimentary Geology, v. 90, p. 213-232.

Nesbitt, H.W., and Young, G.M. (1982), Early Proterozoic climate and plate motions inferred from major element chemistry of lutites. Nature, v. 299, p. 715-717.

Nesbitt, H.W., and Young, G.M. (1984), Formation and diagenesis of weathering profiles. Journal of Geology, v. 97, p. 129-147.

Ozyurt, M., Kirmaci, M.Z., Al-Aasm, I., Hollis, C., Tasli K., and R. Kandemir, R. (2020), REE Characteristics of Lower Cretaceous Limestone Succession in Gumushane, NE Turkey: Implications for ocean paleoredox conditions and diagenetic alteration. Minerals, v. 10, 683. doi:10.3390/min10080683.

Pandey, S., Parcha, S.K., and Srivastava, P.K. (2019), Petrography and geochemistry of the Neoproterozoic sedimentary rocks from the Batal Formation of Spiti Basin: implication on provenance. Arabian Journal of Geosciences, v. 12, 61. doi.org/10.1007/s12517-018-4189-8.

Pirajno, F. (1992), Hydrothermal Mineral Deposits. Springer-Verlag Berlin Heidelberg, p. 1-709.

Pirajno, F., and Joubert, B.D. (1993), An overview of carbonate-hosted mineral deposits in the Otavi Mountain Land, Namibia: implications for ore genesis. Journal of African Earth Sciences, v. 16, p. 265–272.

Pokrovsky, O.S., and Schott, J. (2001), Kinetics and Mechanism of Dolomite Dissolution in Neutral to Alkaline Solutions Revisited. American Journal of Science, v. 301, p. 597-626.

Qing, H., and Mountjoy, E.W. (1994), Rare earth element geochemistry of dolomites in the Middle Devonian Presqu'ile barrier, Western Canada Sedimentary Basin: implications for fluid-rock ratios during dolomitization. Sedimentology, v. 41, p. 787-804.

Reed, C.P., and Wallace, M.W. (2004), Zn-Pb mineralisation in the Silvermines district, Ireland: a product of burial diagenesis. Mineralium Deposita, v. 39, p. 87-102.

Roberts, J.A., Kenward, P.A., Fowle, D.A., Goldstein, R.H., Gonzalez, L.A., and Moore, D.S. (2013), Surface chemistry allows for abiotic precipitation of dolomite at low temperature. Proceedings of the National Academy of Sciences, 110(36), p. 14540-14545.

Rosenberg, P.E., and Holland, H.D. (1964), Calcite-dolomite-magnesite stability relations in solutions at elevated temperatures. Science, v. 145, p. 700-701.

Rosenberg, P.E., Burt, D.M., and Holland, H.D. (1967), Calcite-dolomite-magnesite stability relations in solutions: the effect of ionic strength. Geochimica et Cosmochimica Acta, v. 31, p. 391-396.

Roser, B.P., and Korsh, R.J. (1986), Determination of tectonic setting of sandstone-mudstone suites using SiO_2 content and K_2O/Na_2O ratio. Journal of Geology, v. 94, p. 635-650.

Roser, B.P., and Korsh, R.J. (1988), Provenance signatures of sandstone-mudstone suites determined using discriminant function analysis of major element data. Chemical Geology, v. 67, p. 119-139.

Rudnick, R.L., and Gao, S. (2003), The Composition of the Continental Crust. In: Holland, H.D. and Turekian, K.K. (ed.), Treatise on Geochemistry, Vol. 3, The Crust, Elsevier-Pergamon, Oxford, 1-64. http://dx.doi.org/10.1016/b0-08-043751-6/03016-4.

Sachan, H.K. (1993), Early-replacement dolomitization and deep-burial modification and stabilization: a case study from the Late Precambrian of the Zawar area, Rajasthan (India). Carbonates and Evaporites, v. 8, p. 191-198.

Sahoo, J., Sahoo, P.R., Khan, I., and A. S. Venkatesh, A.S. (2022), Insights into the Metallogenesis of the Felsic Volcanic Hosted Mundiyawas-Khera Cu Deposit, Alwar Basin, Western India. Minerals, v. 12(3), 370. https://doi.org/10.3390/min12030370.

Sajeev, R., Choudhary, S., Konwar, P., Kulshrestha, S.K., and Pandit, D. (2019), Identification of hydrothermal alteration zones for base metal exploration adjoining to Mundiyawas-Khera copper prospect, Rajasthan, India using ASTER data. Indian Journal of Geosciences, v. 73, p. 331-342.

Saller, A.H. (1984), Petrologie and geochemical constraints on the origin of subsurface dolomite, Enewetak Atoll: an example of dolomitization by normal seawater. Geology, v. 12, p. 217-220.

Sarangi, S., Mohanty, S.P., and Barik, A. (2017), Rare earth element characteristics of Paleoproterozoic cap carbonates pertaining to the Sausar Group, Central India: Implications for ocean paleoredox conditions. Journal of Asian Earth Sciences, v. 148, p. 31-50.

Severmann, S., Mills, R.A., Palmer, M.R., and Fallick, A.E. (2004), The origin of clay minerals in active and relict hydrothermal deposits. Geochimica et Cosmochimica Acta, v. 68, p. 73–88.

Seward, T.M., Williams-Jones, A.E., and Migdisov, A.A. (2014), The chemistry of metal transport and deposition by ore-forming hydrothermal fluids. In: Turekian, K., and Holland, H.D. (ed.), Treatise on Geochemistry, Elsevier Science, http://dx.doi.org/10.1016/B978-0-08-095975-7.01102-5.

Sibley, D.F., Dedoes, R.E., and Bartlett, T.R. (1987), Kinetics of dolomitization. Geology, v. 15, p. 1112-1114.

Singh, S.P. (1984), Fluvial sedimentation of the Proterozoic Alwar Group in the Lalgarh graben, northwestern India. Sedimentary Geology, v. 39, p. 95-119.

Singhal, S., Mukherjee, P.K., Saini, N.K., Dutt, S., and Kumar, R. (2019), Effect of carbon on major element analysis of carbonaceous silicate rocks by WD-XRF: An evaluation of error and its correction. Geochemistry: Exploration, Environment, Analysis, v. 19, p. 31-38. https://doi.org/10.1144/geochem2017-077.

Siyi, F., Chenggong, Z., Hondge, C., Anqing, C., Junxing, Z., Zhongtang, S., Shuai, Y., Guo, W., and Wentian, M. (2019), Characteristics, formation and evolution of pre-salt dolomite reservoirs in the fifth member of the Ordovician Majiagou Formation, mid-east Ordos Basin, NW China. Petroleum Exploration and Development, v. 46, p. 1153-1164.

Skinner, B.J. (1979), The many origins of hydrothermal mineral deposits. Ed. by H. L. Barnes Geochemistry of hydrothermal ore deposits, John Wiley & Sons, New York, pp 3–21.

Smyth, H.R., Morton, A., Richardson, N., and Scott, R.A. (2014), Sediment provenance studies in hydrocarbon exploration and production: an introduction. Geological

Society, London, Special Publications, v. 386, 1–6. http://dx.doi.org/10.1144/SP386.21.

Srivastava, V., and Prakash, D. (2020), Preliminary geological investigation for poly-metallic deposits in Khera North Block (Thanaghazi), Alwar district, Rajasthan. Journal of Scientific Research, v. 64, p. 58-65. doi: 10.37398/JSR.2020.640207.

Surya Prakash, L., Ray, D., Paropkari, A.L., Mudholkar, A.V., Satyanarayanan, M., Sreenivas, B., Chandrasekharam, Kota, D., Kamesh Raju, K.A., Kaisary, S., Balavam, V., and Gurav, T. (2012), Distribution of REEs and yttrium among major geochemical phases of marineFe–Mn-oxides: Comparative study between hydrogenous and hydrothermal deposits. Chemical Geology,v. 312-313, p. 127–137.

Taylor, S.R., and McLennan, S.M. (1985), The continental Crust: its Composition and Evolution. Blackwell Scientific Publications, Oxford, p. 1-312.

Tucker, M.E. (1982), Precambrian dolomites: petrographic and isotopic evidence that they differ from Phanerozoic dolomites. Geology, v. 10, p. 7-12.

Turchyn, A.V., Bradbury, H.J., Walker, K., and Sun, X. (2021), Controls on the Precipitation of Carbonate Minerals Within Marine Sediments. Frontiers in Earth Science, 9, 618311. doi: 10.3389/feart.2021.618311.

Vandeginste, V., Snell, O., Hall, M.R., Steer, E., and Vandeginste, A. (2019), Acceleration of dolomitization by zinc in saline waters. Nature Communications, v. 10, 1851. https://doi.org/10.1038/s41467-019-09870-y

Varol, B., and Magaritz, M. (1992), Dolomitization, time boundaries and unconformities: examples from the dolostone of the Taurus Mesozoic sequence, south-central Turkey. Sedimentary Geology, v. 76, p. 117–133.

Von Damma, K.L., Lilley, M.D., Shanks III, W.C., Brockington, M., Bray, A.M., O'Grady, K.M., Olson, E., Graham, A., Proskurowski, G. (2003), the SouEPR Science Party (2003), Extraordinary phase separation and segregation in vent fluids from the southern East Pacific Rise. Earth and Planetary Science Letters, v. 206, p. 365-378.

Warren, J. (2000), Dolomite: occurrence, evolution and economically important associations. Earth Science Reviews, v. 52, p. 1–81.

Wen, H., Zheng, R., Geng, W., Fan, M., and Wang, M. (2007), Characteristics of rare earth elements of lacustrine exhalative rock in the Xiagou formation of lower Cretaceous in Qingxi sag. Jiuxi basin. Frontiers of Earth Science in China, v. 1(3), p. 333-340. doi 10.1007/s11707-007-0040-3.

Wheatley, C.J.R., Friggens, P.J. and Dooge, F. (1986), The Bushy Park carbonate-hosted zinc-lead deposit Griqualand West. In: Anhaeusser, C.R., and Maske, S. (ed.), Mineral Deposits of Southern Africa, Geological Society of South Africa, Johannesburg, p. 891-900.

Wilson, A.M., Sanford, W., Whitaker, F., and Smart, P.

(2001), Spatial patterns of diagenesis during geothermal circulation in carbonate platforms. American Journal of Science, v. 301, p. 727-752.

Wood, S.A., and Samson, I.M. (1998), Solubility of ore minerals and complexation of ore metals in hydrothermal solutions. Eb. by J. P. Richards and P. B. Larson, Techniques in Hydrothermal Ore Deposits Geology, Reviews in Economic Geology, v. 10, p. 33-80.

Wronkiewicz, D.J., and Condie, K.C. (1987), Geochemistry of Archean shales from the Witwatersrand Supergroup, South Africa: Source-area weathering and provenance. Geochimica et Cosmochimica Acta, v. 51, p. 2401-2416.

Zhang, W., Guan, P., Jian, X., Feng, F., and Zou, C. (2014), In situ geochemistry of Lower Paleozoic dolomites in the northwesternTarim basin: Implications for the nature, origin, and evolution of diagenetic fluids. Geochemistry, Geophysics, Geosystems, v. 15, p. 2744–2764, doi:10.1002/2013GC005194.

Zhang., S., Liu, Y.-Q., Li, H., Jiao, X., and Zhou, D.-W. (2020), Hydrothermal-sedimentary dolomite – a case from the Middle Permian in eastern Junggar Basin, China. Journal of Palaeogeography, v. 9, 24. https://doi.org/10.1186/s42501-020-00070-0.

Zotov, A.V., Kudrin, A.V., Levin, K.A., Shikina, N.D., and Var'yash, L.N. (1994), Experimental studies of the solubility and complexing of selected ore elements (Au, Ag, Cu, Mo, As, Sb, Hg) in aqueous solutions. In: Shmulovich, K.I., Yardley, B.W.D., and Gonchar, G.G. (ed.), Fluids in the Crust, Chapman & Hall and Springer, Dordrecht, p. 95-137. https://doi.org/10.1007/978-94-011-1226-0_5.